Ab initio LSDA+U Study of Optical Properties of RVO_4 (R = Eu, Ho, Lu) Compounds

Boualem Merabet[a,b]*, Hatem Alamri[c], Ali Zaoui[a], S. Kacimi[1], Moez Bejar[d], Essebsi Dhahri[d]

[a]*Laboratoire de Physique Computationnelle des Matériaux, Université Djillali Liabès de Sidi Bel-Abbès, Sidi Bel-Abbès, 22000, Algeria*
[b]*Université Mustapha Stambouli, Faculté de Sciences et de la Technologie, Mascara, 29000, Algeria*
[c]*Umm Al-Qura University, Physics Department-University College, Makkah, Saudi Arabia*
[d]*Laboratoire de Physique Appliquée, Faculté des Sciences, Université de Sfax, B.P. 1171, 3000 Sfax, Tunisia*

A first principles investigation at the pressure 7 GPa of the optical properties of RVO_4 (R= Eu, Ho, Lu) orthovanadates in the framework of the density functional theory (DFT) using the linearized-augmented plane-wave method is reported in order to predict new optical materials fo r continuous-wave lasers. The electronic structure of all orthovanadates is studied in zircon-type structure. DFT+U (Hubbard parameter found to be 8eV) calculations predict an antiferromagnetic and nonmagnetic insulating ground states -at ambient conditions- for ($EuVO_4$, $HoVO_4$) and $LuVO_4$, respectively. The results show that these vanadates can be good candidates for laser-host materials, and indicate the possibility of material design to optimize the laser-host materials. The rare-earth ion-doped crystals could enhance the laser performances and improve the isolation characteristic of the optical isolators.

1. Introduction

Besides to be used in a number of applications as thermophosphors, cathodoluminescent materials, scintillators,[1] lithium ion batteries, photocatalysis materials,[2] as alternative green technologies through applications like photocatalytic hydrogen production[3] (and potential applications in renewable energy[4]), the orthovanadates RVO_4 (R is a rare earth trivalent element), exhibiting properties like luminescence, chemical stability, and non-toxicity,[5] have lately appeared as promising optical materials for birefringent solid-state laser applications[6,7] as laser-host materials for continuous-wave lasers[8,9] and biomedical applications as nanoparticles.[10] RVO_4 compounds acting as direct-gap semiconductors (SCs) under compression, exhibit wide optical transparency and large birefringence, being potential candidates for optical isolators, circulators beam displacers and components for polarizing optics.[11] Most of RVO_4 crystallize in a tetragonal zircon-type structure (space group:$I4_1/amd$, Z=4) at room temperature,[1-8] (with 42m as symmetry of the R sites)[12] that consists of isolated VO_4 tetrahedra which surround the R atom to form RO_8 triangular dodecahedra (*i.e.*, Vanadium is tetrahedrally coordinated while the trivalent R cation is coordinated to eight oxygen atoms forming a bidisphenoid).[13]

In solid-state physics, antiferromagnetic phase transition due to the magnetic moments of the rare-earth ions[14] and structural phase transition due to the Jahn-Teller (JT) effect at low temperatures[15] have been studied for RVO_4. R zircons are known to be archetype JT compounds, a number of

which (Dy, Tb, Tm, Tb)VO_4 exhibit spontaneous tetragonal -orthorhombic transitions.[16] Like other ABO_4 oxides, intensive studies have been carried out on the structural evolution of RVO_4 compounds under high-pressure (HP) in order to understand their mechanical properties and HP structural phase transitions; it was found that compression is an efficient tool to improve understanding the main physical properties of vanadates.[17,18]

D. Errandonea *et al*.[19] performed room temperature angle-dispersive x-ray diffraction measurements on zircon-type $EuVO_4$ and $LuVO_4$ under pressure ≤27 GPa, and reported the occurrence of two post-zircon phase transitions near 8 and 21 GPa, respectively. Alka B Garg *et al*.[20] performed such measurements and *ab-initio* calculations (with fully agreement) on $HoVO_4$ ≤28 GPa under quasi-hydrostatic conditions and reported that an irreversible zircon-scheelite transition was found at 8.2 GPa. On another hand and due to the importance of RVO_4 crystals growth with good and large dimensions, several methods have been reported, like the Czochralski process, slow cooling from solution, top-seeded solution growth, laser-heated pedestal growth method, floating-zone (FZ) method and micro-FZ method.[21-26] For example, the importance of YVO_4 (Y: Yttrium) originates from the fact that though Nd lasers was marginal for decades because of serious problems encountered during the growth of YVO_4 crystals by the costly Czochralski method,[27] but the increasing demand for compact, low cost devices has raised the interest for single crystal fibers whose advantage is that they can be successfully used for the construction of high efficiency miniature lasers with single mode

*e-mail: boualem19985@yahoo.fr

emission.[16] Moreover, integrated optical isolators ensure a stable emission of SC lasers in which the nonreciprocity of the magneto-optical (MO) effects plays a key role in the isolation process.[28-30] MO effects, indeed, can be enhanced by incorporating one-dimensional SC photonic crystals integrating lasers & isolators, so as high-performance low-cost devices may be realized.[31] In this trend, doped (Y, Gd) VO_4 have been largely studied as near-IR laser materials due to their higher cross sections, polarized emissions and larger Nd^{3+} incorporation.[16,32] So, in what way are RVO_4 of interest for continuous-wave lasers and optical isolators? Although the optical properties of some of these orthovanadates have been extensively studied, aimed at their application to optical devices, in the form of fluorescent materials, polarizers and laser hosts, there is no first principles studies of optical properties, to the best of our knowledge, of orthovanadates $EuVO_4$, $HoVO_4$ and $LuVO_4$ reported yet. Describing the medium response to an applied electromagnetic radiation within the framework of linear response theory, the optical properties of a material change or affect the characteristics of light passing through it by modifying its propagation vector or intensity. Important relations between the real and imaginary parts of the complex response functions are given first by Kramers[33-34] and Kronig.[35,36] Experimentally, convenient optical measurements involve passing monochromatic light through a thin sample, and measuring the transmitted intensity as a function of wavelength, by using a simple spectrophotometer.[37]

The optical properties, described in terms of the optical dielectric function, are of great importance to design and analysize optoelectronic devices such as light sources and detectors.[38] At all photon energies E = ℏω (ω is the frequency) the imaginary part $\varepsilon_2(\omega)$, which is an essential quantity indicating the various interband transitions in a SC, of the complex dielectric function $\varepsilon(\omega) = \varepsilon_1(\omega) + i\,\varepsilon_2(\omega)$, is strongly related to the joint density of states and optical matrix elements,[38] and the real part $\varepsilon_1(\omega)$ is derived from $\varepsilon_2(\omega)$. There are two contributions to $\varepsilon(\omega)$, interband and intraband transitions. We neglect the *indirect* interband transitions which involve scattering of phonons and are expected to give a small contribution to $\varepsilon(\omega)$.[39]Our purpose here, is to report the optical properties of the three vanadates in the light of *ab initio* calculations under a fixed pressure of ~7 GPa, in order to facilitate a much deeper understanding of these properties for the whole family of vanadates. The paper is organized as follows: After a theoretical approach overview given in Section 2, results and discussions are presented in Section 3, and then a conclusion is provided in Section 4.

2. Computational Method

The calculations are based on the DFT implemented in the WIEN2k code.[40] The atoms were represented by hybrid full-potential (FP) *linear* augmented plane-wave plus local orbitals (L/APW+*lo*) method,[41] where wave functions, charge density and potential are expanded in spherical harmonics within no overlapping muffin-tin (MT) spheres, and plane waves are used in the remaining interstitial region of the unit cell. In this code, core and valence states are treated differently. Core states are treated within a multiconfiguration relativistic Dirac-Fock approach, while valence states are treated in a scalar relativistic approach. Exchange-correlation energy was calculated using DFT+*U* approach, processed by the local spin density approximation (LSDA).[42] The analysis is done to ensure the total energy convergence in terms of the variational cutoff-energy parameter. On an other hand, we have used an appropriate set of *k* points to compute the total energy. The standard built-in basis functions were applied with the valence configurations of (Eu: $5s^2\,5p^6\,4f^7\,5d^1\,6s^2$), (Ho: $5s^2\,5p^6\,4f^{11}\,5d^1\,6s^2$), (Lu: $5s^2\,5p^6\,4f^{14}\,5d^1\,6s^2$), (V: $3s^2\,3p^6\,3d^3\,4s^2$) and (O: $2s^2\,2p^4$). Total energy were minimized using a set of 150, 163 and 163 *k*-points in the irreducible sector of the Brillouin zone for the orthovanadates $EuVO_4$, $HoVO_4$ and $LuVO_4$ respectively and a value of 7Ry for the cutoff energy was used. Values of 2.5 Bohr for rare earth elements, 1.6 Bohr for Vanadium and 1.45 Bohr for Oxygen have been adopted as MT radii. The plane wave cut off parameters $R_{MT}.K_{max}$ and G_{max} are taken to be respectively 7 and 12 for optimization and analyzing various properties of all vanadates; *l*- maximum (l_{max}) value of 12 is considered. To calculate the exchange-correlation energy describing the strong on-site correlation between the 4*f* electrons, we added the above-mentioned effective Coulomb interaction *U*, so that *U* in an atom corresponds to of the unscreened Slater integrals (F_0).[43] The effective U (U_{eff}) can be estimated by constraint DFT calculations, where some valence electrons are selectively treated as core electrons to switch off any hybridization with other electrons. Due to screening, U_{eff} in solids is much smaller than F_0 for atoms. The number of electrons in this non-hybridizing *f*-shell was varied and F_{eff}^0 was then calculated from[43]

$$F_{eff}^0 = \varepsilon_{4f\uparrow}\left(\frac{n+1}{2}, \frac{n}{2}\right) - \varepsilon_{4f\uparrow}\left(\frac{n+1}{2}, \frac{n}{2} - 1\right) - \varepsilon_F\left(\frac{n+1}{2}, \frac{n}{2}\right) + \varepsilon_F\left(\frac{n+1}{2}, \frac{n}{2} - 1\right),$$

where $\varepsilon_{4f\uparrow}$ stands for the 4*f* spin-up eigenvalue of rare earth atoms. An U of 8 eV should ensures the strong Coulomb repulsion (a correlation effect) between *f*-electrons pushing these states far from the Fermi level (E_F) and the degeneracy between different *f* orbits would be lifted.

Optical properties of the materials are determinated by the complex dielectric function $\varepsilon(\omega)$. It's well known that all optical properties of the medium are depicted well by the frequency dependent dielectric function and that using LDA to the DFT usually leads to underestimate the energy bandgap (E_g) and lattice constant in SCs. This underestimation is mainly due to the fact that the LDA functional is based on

simple model assumption which is not sufficiently flexible for accurate reproduction of the exchange correlation energy and its charge derivative. To avoid this shortcoming, a scissors operation with a rigid upward shift of the conduction band has been used to correct E_g that LDA underestimates, although the DFT has proven to be one of the most accurate theories for the computation of the electronic structure of solids.[44-49]

3. Results and Discussion

The electronic properties of a SC are primarily determined by intraband transitions, which describe the transport of carriers in real space. Optical properties are meanwhile connected with these interband transitions, so as a strict separation is impossible. Hence, the optical and electronic SC properties are intimately related and should be discussed jointly.[50] Fig. 1 shows that $\varepsilon_2(\omega)$ is characterized by a single peak structure (beyond E_g) for $EuVO_4$ and $HoVO_4$ (under 7 GPa, ε_2^{xx}): $E_1 =$ 3.898 and 4.067 eV respectively, and a two peak structure for $LuVO_4$ (under 7 GPa, ε_2^{zz}): (E_1, E_2)=3.977, 4.909 eV. In order to well understand optical transitions phenomena in our SC vanadates, we give in Table 1 the peaks of the dielectric function $\varepsilon_2(\omega)$, static optical parameters $\varepsilon_1(0)$ and

refractive indices n^{zz} at 5.67 eV near up limit of an energy range experimentally exploited, compared to the available data in literature.

3.1 Refractive index and extinction coefficient

The two most important optical properties of the material are its refractive index n and extinction coefficient (or attenuation index) k. n, the most interesting optical constant, depends in general on the wavelength of the electromagnetic wave, through *dispersion* relations denoting frequency or wavelength dependence of n and k. In materials where an electromagnetic wave can lose its energy during its propagation, the refractive index becomes complex (N). Real and imaginary parts of N (n; k, respectively[37], are usually used for the propagation and dissipation of electromagnetic waves in a medium.[51]) Given the material parameters such as $\varepsilon(\omega)$, the conductivity $\sigma 1$, and the permeability $\mu 1$ denoting the charge of the electric and magnetic fields and current when matter is present, N as a response function describing optical properties of the medium is defined as follows[51]

$$\overline{N} = n + ik = \left[\varepsilon_1 \mu_1 + i\frac{4\pi\mu_1\sigma_1}{\omega}\right]^{1/2} = [\overline{\varepsilon}\,\mu_1]^{1/2} \qquad (1)$$

where n and k are completely determined by σ_1, μ_1, and ε_1[51]

$$\overline{n}^2 = \frac{u_1}{2}\left\{\left[\varepsilon_1^2 + \left(\frac{4\pi\sigma_1}{\omega}\right)^2\right]^{1/2} + \varepsilon_1\right\} \text{and } \overline{k}^2 = \frac{u_1}{2}\left\{\left[\varepsilon_1^2 + \left(\frac{4\pi\sigma_1}{\omega}\right)^2\right]^{1/2} - \varepsilon_1\right\} \,(2)$$

These two important relations contain all the information on the electromagnetic wave propagation in the material. ε_1, μ_1, and σ_1 are given in terms of n and k:

$$n^2 - k^2 = \varepsilon_1\mu_1 \text{ and } 2nk = \frac{4\pi\mu_1\sigma_1}{\omega} \qquad (3)$$

and the complex refractive index, given in eq.(1), can be written:

$$\overline{N}^2 = \mu_1\left[\varepsilon_1 + i\frac{4\pi\sigma_1}{\omega}\right] = \mu_1\overline{\varepsilon} \simeq \frac{4\pi i\mu_1\overline{\sigma}}{\omega}$$
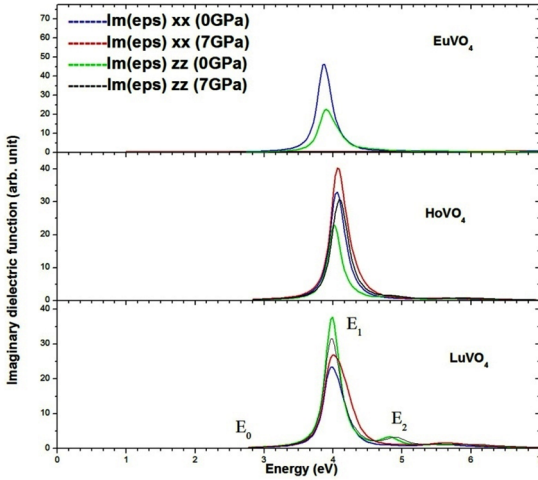$$\overline{N}^2 = \mu_1\left[\varepsilon_1 + i\frac{4\pi\sigma_1}{\omega}\right] = \mu_1\overline{\varepsilon} \simeq \frac{4\pi i\mu_1\overline{\sigma}}{\omega} \qquad (4)$$

Figure 1. Imaginary part of ε^{xx}, ε^{zz} of $EuVO_4$, $HoVO_4$ and $LuVO_4$, under 0 and 7 GPa.

Table 1. Calculation of the peaks in the dielectric function $\varepsilon_2(\omega)$, static optical parameters $\varepsilon_1(0)$, refractive indices n, and available data from literature, for $EuVO_4$, $HoVO_4$ and $LuVO_4$ (under 7GPa).

Compound	E_0^{xx}(eV)E_0^{zz}	E_1^{xx}(eV)E_1^{zz}	E_2^{xx}(eV)E_2^{zz}	$\varepsilon_1^{xx}(0)$ $\varepsilon_1^{zz}(0)$	n
$EuVO_4$	2.871[a]2.898[a]	3.898[a]3.933[a]	– –	12.13[a]17.63[a]	2.18[a]
Exp/th.works	– –	– –	– –	– –	~2–2.3[b]
$HoVO_4$	2.816[a]3.062[a]	4.071[a]4.091[a]	– –	9.71[a]7.72[a]	2.15[a]
Exp/th.works	– –	– –	– –	– –	~2–2.3[b]
$LuVO_4$	2.653[a]2.955[a]	4.001[a]3.977[a]	– 4.909[a]	10.01[a]10.19[a]	1.96[a]
Exp/th.works	– –	– –	– –	– –	~2–2.3[b]

[a] This work, n is given at 5.67 eV according to *zz*;

[b] The large n that exhibit RVO_4 from Ref. [52].

As mentioned above, the refractive index $n(\omega)$ of a SC is a very important physical parameter related to the microscopic atomic interactions; its knowledge turns out to be of fundamental importance in optoelectronics.[39] The crystal can be considered as a collection a of electric charges, and $n(\omega)$ will then be related to the local polarization of these quantities. It can be described in terms of the complex dielectric function as[39]

$$n(\omega) = \frac{\sqrt{\varepsilon_1(\omega) + \sqrt{\varepsilon_1^2(\omega) + \varepsilon_1^2(\omega)}}}{\sqrt{2}} \quad (5)$$

with regard to k:

$$k(\omega) = \frac{\sqrt{-\varepsilon_1(\omega) + \sqrt{\varepsilon_1^2(\omega) + \varepsilon_1^2(\omega)}}}{\sqrt{2}} \quad (6)$$

In Fig. 2, we present n (7 GPa) over a range experimentally exploited ≤ 6 eV, where the dispersion is normal. Experimentally, RVO4 exhibit large refractive indices (~2-2.3), a birefringence ~0.22, and effectively no IR absorption (1.5-2.5μm).([52]) Here according to zz, a common photon energy around 5.7 eV corresponds to a refractive index about 2.

3.2 Reflectivity

Although measuring experimentally the reflectivity (R) of a radiation incident normally on a semi-infinite slab of an absorbing material is easy,[53]-[55] a direct calculation of such optical constant can be alternatively obtained by the Kramers-Kronig analysis of data.[33]-[36] It's more essential noting here that absolute reflectivities should be known accurately. This approach has largely been used when the reflection spectrum is more complex, as in the ultraviolet region, and R is related N to by eq.(7). In analogy with the situation of a nonabsorbing medium where $n = \varepsilon^{1/2}$ (both n and ε are real), in an absorbing medium the same relation can be used with both N and $\overline{\varepsilon}$ complex, where n is the ordinary index of refraction and k is the extinction coefficient. The

optical reflectivity R(ω) in the special configuration of normal inci dence can be expressed as

$$R(\omega) = \left| \frac{1 - \overline{N}}{1 + \overline{N}} \right|^2 = \left| \frac{(\varepsilon_1(\omega) + i\varepsilon_2(\omega))^{1/2} - 1}{(\varepsilon_1(\omega) + i\varepsilon_2(\omega))^{1/2} + 1} \right|^2 = \frac{(1-n)^2 + k^2}{(1+n)^2 + k^2} \quad (7)$$

For a dielectric material without losses, $k \to 0$; the normal-incidence reflectivity is solely deter mined by the refractive index n:

$$R(\omega) = \left(\frac{1-n}{1+n} \right)^2 \quad (8)$$

and it can approach unity if n is large. This other very important parameter (inferred from n) characterizes the reflective energy part of the interface of a solid, and depends on an incident photon energy. Main peaks in R(ω) spectrum are corresponding to interband transitions.[37] Fig. 3 shows the behavior of R(ω) in dependance on the photon energy for the three compounds. Corresponding to interband transitions the main peaks in R(ω) spectrum are respectively 71.16, 75.65 and 68.95% at 1.565, 1.809 and 1.701 eV, for EuVO$_4$, HoVO$_4$ and LuVO$_4$ (under 7 GPa, according to xx) and decreases by increasing energy. According to zz, a photon energy ~5.7eV yields a reflectivity of 0.16, implying k of the same order corresponding to an absorption coefficient (given in more details below) larger than 2.5×10^5 cm^{-1}.

3.3 Optical conductivity

Complex dielectric constants $\overline{\varepsilon} = \varepsilon_1 + i\frac{4\pi\sigma_1}{\omega} = \varepsilon_1 + i\varepsilon_2$ and optical conductivities $\overline{\sigma} = \sigma_1 + i\sigma_2$ are related to each other through

$$\overline{\varepsilon} = 1 + \frac{4\pi i}{\omega}\overline{\sigma} \gg 1 \Rightarrow \sigma(\omega) = -\frac{i\omega}{4\pi}\varepsilon(\omega)$$
$$\overline{\varepsilon} = 1 + \frac{4\pi i}{\omega}\overline{\sigma} \gg 1 \Rightarrow \sigma(\omega) = -\frac{i\omega}{4\pi}\varepsilon(\omega) \quad (9)$$

We have calculated σ(ω) over an energy range $\leq$15eV. In Fig. 4, we show the σ(ω) spectra where several peaks corresponding to the bulk plasmon exitations, caused by electrons crossing from the valence to the conduction band, are represented. Values of σ(ω) in the high energy range (beyond 5 eV) and the low energy range (0.484-4.34 eV) are corresponding to interband and intraband transitions, respectively. There is a single sharp peak in the low energy range and several small ones in the high energy range for all RVO$_4$ compounds. The main peaks positions are localized at 1.511, 1.264 and 1.236 eV (0 GPa) and 1.201, 1.257 and 1.286 eV (under 7 GPa, according to xx) for EuVO$_4$, HoVO$_4$ and LuVO$_4$, respectively.

3.4 Electron energy loss function

The electron energy-loss function, L(ω), describes an interaction by which energy is lost by a fast moving electron
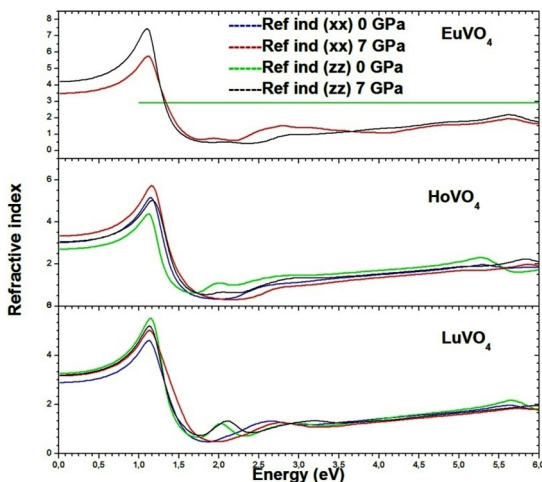
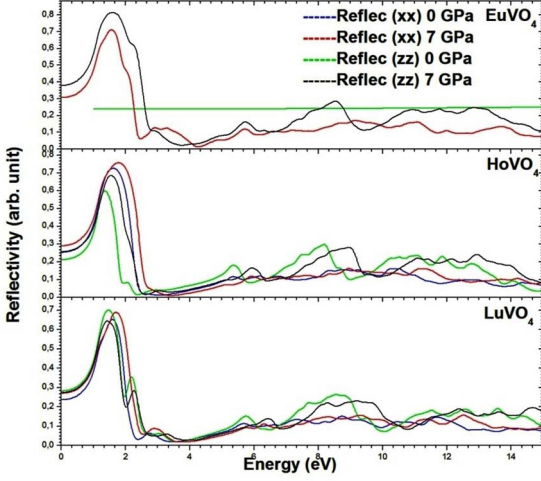**Figure 2.** Refractive indices n^{xx}, n^{zz} of EuVO$_4$, HoVO$_4$ and LuVO$_4$, under 0 and 7 GPa.

Figure 3. Reflectivity R^{xx}, R^{zz} of $EuVO_4$, $HoVO_4$ and $LuVO_4$, under 0 and 7 GPa.

Figure 4. Optical conductivity σ^{xx}, σ^{zz} of $EuVO_4$, $HoVO_4$ and $LuVO_4$, under 0 and 7 GPa.

Figure 5. Energy loss of L^{xx}, L^{zz} of $EuVO_4$, $HoVO_4$ and $LuVO_4$, under 0 and 7 GPa.
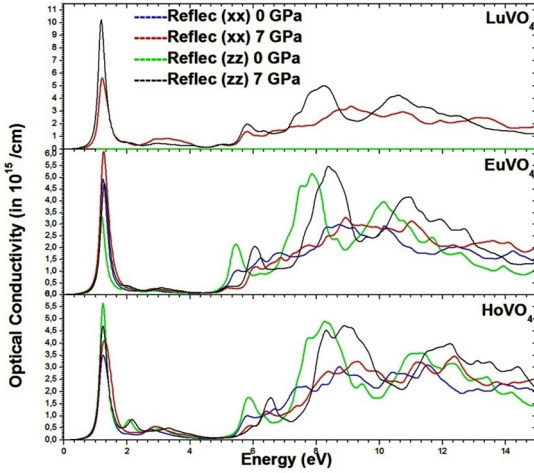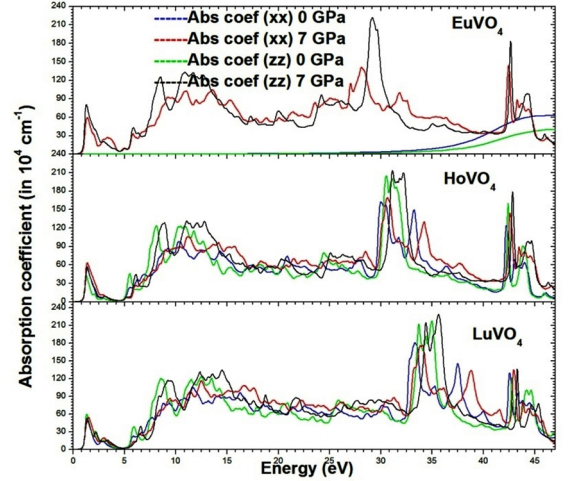

Figure 6. Absorption coefficient α^{xx}, α^{zz} of $EuVO_4$, $HoVO_4$, $LuVO_4$, under 0 and 7 GPa.

travelling throughout the material. Interactions may include phonon excitation, interband and intraband transitions, plasmon excitations, inner shell ionizations and Cerenkov radiations. If both parts of $\sigma(\omega)$ are such as $\sigma_1 \gg |\sigma_2|$, R →1. $L(\omega)$ of fast electrons moving in the medium, usually large at the plasma frequency, is [56]

$$L(\omega) = \text{Im}\left[-1/\varepsilon(\omega)\right] = \frac{\varepsilon_2(\omega)}{\varepsilon_1^2(\omega) + \varepsilon_2^2(\omega)} \quad (10)$$

This function is the basic parameter measured by the electron loss spectroscopy. The most prominent peak in $L(\omega)$ is identified as the plasmon peak, signaling the energy of collective excitations of the electronic charge density in the crystal. As displayed in Fig. 5, the highest peak positions for $L^{xx}(\omega)$ were calculated at 2.308, 2.519 and 2.298 eV (7 GPa), and 2.445, 2.256 and 2.117 eV (0 GPa), respectively for $EuVO_4$, $HoVO_4$ and $LuVO_4$. The sharp maximum in $L(\omega)$ is refered to an existence of plasma oscillations. In comparison to the other

physical quantities, the main peaks of $L(\omega)$ are clear and allow a good distinction between both 0 GPa and 7 GPa spectra.

3.5 Absorption coefficient

The absorption related to the transitions between the occupied and unoccupied states is caused by excitations due to the interaction of photons and electrons. Optical absorption is due to the interband and intraband transitions (Drude term).[57] The peaks position in absorption spectrum corresponds to peaks of $\varepsilon_2(\omega)$. Using both parts of $\varepsilon(\omega)$, the optical absorption coefficient $\alpha(\omega)$ that characterizes such phenomenon, is defined as the light energy absorbed in unit length per unit incident energy[57]

$$\alpha(\omega) = \frac{\sqrt{2}\,\omega}{c}\left[(\varepsilon_1^2(\omega) + \varepsilon_2^2(\omega))^{1/2} - \varepsilon_1(\omega)\right]^{1/2} = \frac{4\pi}{\lambda}k(\omega) \quad (11)$$

where c and λ are respectively the velocity and wavelength of light in the vacuum. The light incident on $R(VO_4)$ active layers may cause excitation of the ground state electrons from the valence band to the conduction band or from one subband to a higher sub-band, where the required energy is supplied by photons and the light is then absorbed.[58]

Fig. 6 shows that at low energies (≤ 26.7, 29.48 and 32.46 eV for $EuVO_4$, $HoVO_4$ and $LuVO_4$, respectively), the contributions of the absorption spectra may be related to the transition between energy levels in bands which are very close to each other, and thus leads to the broadening of such spectra. Zero absorption α^{xx} and α^{zz} are observed for photons possessing energies below E_g for all RVO_4, while first oscillations at ~1.31 eV, due to interband transitions, are apparent related to the peaks 81.63×10^4, 55.72×10^4 and 51.87×10^4 cm$^{(-1)}$ respectively for $EuVO_4$, $HoVO_4$ and $LuVO_4$ (7GPa, according to zz). Beyond first peaks, other ones appear and could be due to the R atoms nature. At higher energies, the absorption due to valance-to-conduction band transitions, is very acute and thus leads to very sharp spectra. As Fig. 6 shows, several α^{zz} peaks appear beyond the above tops of low energies for all RVO_4, witch is expected to show a significant interest in the design of solar cells on a wide range of wavelengths.

4. Conclusion

In this work we presented an ab initio calculation using the FP-LAPW method, in the framework of DFT, to compute $\varepsilon(\omega)$ and other optical parameters of our three RVO_4 compounds. The predicted RVO_4 active layers show powerfully better performances, such as n^{xx} and n^{zz} at the origin. We can say that the zircon type structure of these RVO_4 vanadates may not only be an attractive alternative to the other structures (in particular their counterparts induced by phase transitions under pressure) for designing devices operating by intersub-band transitions such as laser-host materials but also an efficient way of computing the $\varepsilon(\omega)$-related parameters. Our main results show that:

$\varepsilon_2(\omega)$ for $EuVO_4$, $HoVO_4$ behaves similarly with a slight shift and single peak toward high energies under 7 GPa, while for $LuVO_4$ there are two main optical transitions, witch is of great interet for optoelectronics, at 3.977 and 4.894 eV, but under 0 GPa. We mention that $\varepsilon(\omega)$ has a quite different behavior for RVO_4.

n^{xx} and n^{zz} have nonlinear dispersion in high energies range. A large effect of R atoms on RVO_4 facet reflectivities is shown at low energies and high pressure.

σ^{zz} have similar behaviors in low energies (≤ 4.67eV); from 8.3 eV there are several peaks whose the first one is common for all RVO_4, then σ decreases with energy increasing which could be due to the difference between the R cations.

$\alpha(\omega)$ exhibit behaviors totally different, as strongest peaks beyond 26.7 eV and regularly up-shifted energy ranges, for $EuVO_4$, $HoVO_4$ and $LuVO_4$ respectively.

Conflict of interest: The authors declare that no conflict of interest with any part or authority they have.

5. References

1. Dong FQ, Wu QS, Sun DM, Ding YP. Morphology-tunable synthesis of SrWO4 crystals via biomimetic supported liquid membrane (SLM) system. *Journal of Materials Science*. 2008;43(2):641-644.

2. Kalai Selvan K, Gedanken A, Anilkumar P, Manikandan G, Karunakaran C. Synthesis and Characterization of Rare Earth Orthovanadate (RVO4; R = La, Ce, Nd, Sm, Eu & Gd) Nanorods/Nanocrystals/Nanospindles by a Facile Sonochemical Method and Their Catalytic Properties. Journal of Cluster Science. 2009;20(2):291-305.

3. Rakesh K, Khaire S, Bhadge D, Dhanasekaran P, Deshpande SS, Awatwe SV, et al. Role of doping-induced photochemical and microstructural properties in the photocatalytic activity of InVO4 for splitting of water. *Journal of Materials Science*. 2011;46:5466.

4. Errandonea D, Manjón FJ, Muñoz A, Rodríguez-Hernández P, Panchal V, Achary SN, et al. High-pressure polymorphs of TbVO4: A Raman and *ab initio* study. *Journal of Alloys and Compounds*. 2013;577:327-335

5. Errandonea C, Popescu C, Achary SN, Tyagi AK, Bettinelli M. In situ high-pressure synchrotron X-ray diffraction study of the structural stability in NdVO4 and LaVO4. *Materials Research Bulletin*. 2014;50:279-284.

6. Ryba-Romanowski W. YVO4 crystals - puzzles and challenges. Crystal Research and Technology. 2003;38(3-5):225-236.

7. Miyazawa S. Optical crystals survived in information technology systems. Opto-Electronics Review. 2003;11(2):77-84.

8. Chakoumakos BC, Abraham MM, Boatner LA. Crystal Structure Refinements of Zircon-Type MVO4 (M = Sc, Y, Ce, Pr, Nd, Tb, Ho, Er, Tm, Yb, Lu). *Journal of Solid State Chemistry*. 1994;109(1):197-202.

9. Liu H, An Q, Chen F, Vázquez de Aldana JR, del Rosal Rabes B. Continuous-wave lasing at 1.06 µm in femtosecond laser written Nd:KGW waveguides. *Optical Materials*. 2014;37:93-96.

10. Liang Y, Chui P, Sun X, Zhao Y, Cheng F, Sun K. Hydrothermal synthesis and upconversion luminescent properties of YVO4:Yb3+,Er3+ nanoparticles. *Journal of Alloys and Compounds*. 2013;552:289-293.

11. Panchal V, Errandonea D, Segura A, Rodriguez-Hernandez P, Muñoz A, Lopez-Moreno S, et al. The electronic structure of zircon-type orthovanadates: Effects of high-pressure and cation substitution. *Journal of Applied Physics*. 2011;110(4):043723.

12. Wyckoff RWG. *Crystal Structure*. Volume 3. New York: Interscience; 1965.

13. Aldred AT. Cell volumes of APO4, AVO4, and ANbO4 compounds, where A = Sc, Y, La-Lu. *Acta Crystallographica Section B*. 1984;40(Pt 6):569-574.

14. Oka K, Unoki H, Shibata H, Eisaki H. Crystal growth of rare-earth orthovanadate (RVO$_4$) by the floating-zone method. *Journal of Crystal Growth*. 2006;286(2):288-293.

15. Unoki H, Sakudo T. Dielectric Anomaly and Improper Antiferroelectricity at the Jahn-Teller Transitions in Rare-Earth Vanadates. *Physical Review Letters*. 1977;38(3):137-139.

16. Gehring GA, Gehring KA. Co-operative Jahn-Teller effects. *Reports on Progress in Physics*. 1975;38(1):1-90.

17. Gleissner, J, Errandonea, D, Segura, A, PellicerPorres, J, Hakeem, Malik, Proctor, JE, Raju, SV, Kumar, RS, Rodriquez-Hernandez, P, Munoz, A, Lopez-Moreno, S and Bettinelli, M., Monazite type SrCrO$_4$ under compression, *Phys. Rev. B* 2016;94:134108-1 -134108-13

18. Liu M, Lv ZL, Cheng Y, Ji GF, Gong M. Structural, elastic and electronic properties of CeVO$_4$ via first-principles calculations. Computational Materials Science. 2013;79:811-816.

19. Errandonea D, Lacomba-Perales R, Ruiz-Fuertes J, Segura A, Achary SN, Tyagi AK. High-pressure structural investigation of several zircon-type orthovanadates. Physical Review B. 2009;79(18):184104.

20. Garg AB, Errandonea D, Rodríguez-Hernández P, López-Moreno S, Muñoz A, Popescu C. High-pressure structural behaviour of HoVO$_4$: combined XRD experiments and ab initio calculations. Journal of Physics: Condensed Matter. 2014;26(26):265402.

21. Van Uitert LG, Linares RC, Soden RR, Ballman AA. Role of *f*- Orbital Electron Wave Function Mixing in the Concentration Quenching of Eu^{3+}. *Journal of Chemical Physics*. 1962;36(3):702-705.

22. J.J. Rubin, L.G. van Utert, Growth of Large Yttrium Vanadate Single Crystals for Optical Maser Studies, *J. Appl. Phys.* 1966;37:2920-2921.

23. Smith SH, Garton G, Tanner BK. Top-seeded flux growth of rare-earth vanadates. *Journal of Crystal Growth*. 1974;23(4):335-340.

24. Eedei S, Ainger FW. Crystal growth of YVO$_4$ using the LHPG technique. *Journal of Crystal Growth*. 1993;128(1-4, Pt 2):1025-1033.

25. Katsutoshi Muto and Kenzo Awazu, Growth of Yttrium Vanadate Crystal by Modified Floating Zone Technique, Jpn. J. Appl. Phys. 1969;8:1360

26. H. Unoki, K. Oka, N. Kumashiro, Annual Report (**S58**) for Electrotechnical Laboratory, 1984, p. 76.

27. Lisiecki R, Solarz P, Dominiak-Dzik G, Ryba-Romanowski W, Sobczyk M, Cerný P, et al. Comparative optical study of thulium-doped YVO$_4$, GdVO$_4$, and LuVO$_4$ single crystals. *Physical Review B*. 2006;74(3):035103.

28. Levy M, Scarmozzino R, Osgood RM Jr, Wolfe R, Cadieu FJ, Hedge H, et al. Permanent magnet film magneto-optic waveguide isolator. *Journal of Applied Physics*. 1994;75(10):6286.

29. Shimizu H, Tanaka M. Design of semiconductor-waveguide-type optical isolators using the nonreciprocal loss/gain in the magneto-optical waveguides having MnAs nanoclusters. *Applied Physics Letters*. 2002;81(27):5246.

30. Zaets W, Ando K. Optical waveguide isolator based on nonreciprocal loss/gain of amplifier covered by ferromagnetic layer. *IEEE Photonics Technology Letters*. 1999;11(8):1012-1014.

31. Shimizu H, Miyamura M, Tanaka M. Enhanced magneto-optical effect in a GaAs:MnAs nanoscale hybrid structure combined with GaAs/AlAs distributed Bragg reflectors. *Journal of Vacuum Science & Technology B, Nanotechnology and Microelectronics: Materials, Processing, Measurement, and Phenomena*. 2000;18(4):2063

32. de Camargo ASS, Nunes LAO. Nd/sup 3+/doped yttrium and gadolinium orthovanadates crystal fibers for the construction of diode-pumped lasers at 1.06 /spl mu/m. In: *Conference on Lasers and Electro-Optics, 2003 CLEO 2003*; 2003 Jun 6; Baltimore, MD, USA.

33. H. A. Kramers, Some remarks on the theory of absorption and refraction of x-rays, *Nature*. 1926;117:775.

34. Kramers HA. Collected Scientific Papers. Amsterdam: North-Holland; 1956.

35. Kronig RL. On the Theory of Dispersion of X-Rays. *Journal of the Optical Society of America*. 1926;12(6):547-557.

36. Kronig L R. de, General theory of dielectric and magnetic losses, *Ned. Tjidschr. Natuurdk.* 1942;9:402.

37. Tan WC, Koughia K, Singh J, Kasap SO. Optical Properties of Condensed Matter and Applications. In Singh J, ed. *Fundamental Optical Properties of Materials*. Hoboken: John Wiley & Sons; 2006.

38. Adachi S. *Properties of Semiconductor Alloys: Group-IV, III-V and II-VI Semiconductors*. Hoboken: John Wiley & Sons; 2009.

39. Smith NV. Photoelectron Energy Spectra and the Band Structures of the Noble Metals. *Physical Review B*. 1971;3(6):1862.

40. Blaha P, Schwarz K, Madsen GKH, Kvasnicka D, Luitz J. *WIEN2K: An Augmented Plane Wave plus Local Orbitals Program for Calculating Crystal Properties*. Vienna: Vienna University of Technology; 2001.

41. Sjöstedt E, Nordstroöm L, Singh DJ. An alternative way of linearizing the augmented plane-wave method. *Solid State Communications*. 2000;114(1):15-20.

42. Anisimov VI, Zaanen J, Andersen OK. Band theory and Mott insulators: Hubbard *U* instead of Stoner *I*. *Physical Review B*. 1991;44(3):943.

43. Anisimov VI, Gunnarsson O. Density-functional calculation of effective Coulomb interactions in metals. *Physical Review B*. 1991;43(10):7570.

44. Reshak AH, Parasyuk OV, Fedorchuk AO, Kamarudin H, Auluck S, Chyský J. Optical Spectra and Band Structure of AgxGaxGe1-xSe2 (x = 0.333, 0.250, 0.200, 0.167) Single Crystals: Experiment and Theory. *Journal of Physical Chemistry B*. 2013;117(48):15220-15231.

45. Reshak AH, Chen X, Auluck S, Kamarudin H, Chyský J, Wojciechowski A, et al. Linear and Nonlinear Optical Susceptibilities and the Hyperpolarizability of Borate LiBaB$_9$O$_{15}$ Single-Crystal: Theory and Experiment. *Journal of Physical Chemistry B* . 2013;117(45):14141-14150.

46. Reshak AH, Kamarudin H, Kityk IV, Auluck S. Dispersion of Linear, Nonlinear Optical Susceptibilities and Hyperpolarizability of $C_{11}H_8N_2O$ (o-Methoxydicyanovinylbenzene) Crystals. *Journal of Physical Chemistry B*. 2012;116(45):13338-13343.

47. Reshak AH, Kamarudin H, Auluck S. Acentric Nonlinear Optical 2,4-Dihydroxyl Hydrazone Isomorphic Crystals with Large Linear, Nonlinear Optical Susceptibilities and Hyperpolarizability. *Journal of Physical Chemistry B* . 2012;116(15):4677-4683.

48. Davydyuk GE, Khyzhun OY, Reshak AH, Kamarudin H, Myronchuk GL, Danylchuk SP, et al. Photoelectrical properties and the electronic structure of $Tl_{1-x}In_{1-x}Sn_xSe_2$ (x = 0, 0.1, 0.2, 0.25) single crystalline alloys. *Physical Chemistry Chemical Physics*. 2013;15(18):6965-6972.

49. Reshak AH, Kogut YM, Fedorchuk AO, Zamuruyeva OV, Myronchuk GL, Parasyuk OV, et al. Linear, non-linear optical susceptibilities and the hyperpolarizability of the mixed crystals $Ag_{0.5}Pb_{1.75}Ge(S_{1-x}Se_x)_4$: experiment and theory. *Physical Chemistry Chemical Physics* . 2013;15(43):18979-18986.

50. Haug H, Koch SW. *Quantum Theory of the Optical and Electronic Properties of Semiconductors*. London: World Scientific Publishing; 2004.

51. Dressel M, Griner G. Electrodinamics of Solids: Optical Properties of Electrons in Matter. Cambridge: Cambridge University Press; 2001.

52. Guedes I, Hirano Y, Grimsditch M, Wakabayashi N, Loong CK, Boatner LA. Raman study of phonon modes in $ErVO_4$ single crystals. *Journal of Applied Physics*. 2001;90(4):1843-1846.

53. Willardson RK, Beer AC, eds. Semiconductors and Semimetals. Volume 3. Cambridge: Academic Press; 1967.

54. Moss TS, ed. *Optical Properties of Semiconductors*. Chap 2. London: Butterworth; 1959.

55. Spitzer WG, Kleinman DA. Infrared Lattice Bands of Quartz. *Physical Review*. 1961;121(5):1324.

56. Xu M, Wang SY, Yin G, Li J, Zheng YX, Chen LY, et al. Optical properties of cubic Ti_3N4, Zr_3N_4, and Hf_3N_4. *Applied Physics Letters*. 2006;89(15):151908.

57. Romaniello P, de Boeij PL, Carbone F, van der Marel D. Optical properties of bcc transition metals in the range 0-40 eV. *Physical Review B*. 2006;73(7):075115.

58. Nag BR. *Physics of Quantum Well Devices*. Calcutta: Kluwer Academic; 2000.